Soil Behavior and Pile Design: Lesson Learned from Some Prediction Events - Part 1: Aged and Residual Soils

G. Togliani
Geologist, Massagno, Switzerland (gtogliani@bluewin.ch)

ABSTRACT: Pile design methods generally do not consider phenomena such as aging, cementation and weathering, responsible for the presence of microstructures in the soil surrounding the piles and affecting their performance. Some prediction events involving known structured soils are analyzed taking as a reference the CPT-based SBT classification system recently updated by P.K. Robertson (2016). It is shown that the normalized small-strain rigidity index K^*_G can be useful to assess the impact of soil microstructure on pile capacity.

1 INTRODUCTION

The prediction events chosen are Merville (2003) and Porto (2004), locations where at the time of prediction, it was known that soils were aged and residual, respectively, and therefore micro-structured.
Tables summarizing soils and piles characteristics are provided below, while some CPTu plots (Page 2) complete the information as illustration of all the data used for piles design (axial capacity and load-movement curves).

For both sites it is sufficient to observe the CPT SBT I_c and fine contents (FC) curves (Figures 2 and 5) to see how their trend has been influenced by the soil microstructure. In fact, despite the lithological difference, the corresponding I_c curves are quite similar, proving that the Merville Flanders clays show a behaviour at the border to "sand like" soils, whereas, due to very high f_s values, the Porto silty sands are close to behave as "clay like".

Pairs of measured values should be used to calculate K^*_G; however, being too few those of V_s, it is reasonable to refer to derived values since the measured and predicted V_s curves are close enough one to the other (Figures 1 and 4).

Table 1 Merville: Soil and Pile Details

Pile Type and Length:	Driven (IHC S70), 9.4m
Material and Diameter:	Steel Pipe (open ended), 0.508/0.487m
Driving Date:	04.08.2003
Soil Plug Height:	7.27 m
SLT Date:	05.19.2003
Deposit:	Marine (Ypresian)
Lithology:	Clays (50% Smectit, CF=93%)
Soil structure from	Aging, Mechanical OC
GWT, w_n , γ	(-1.5/-1.9m), 32.3%, 18.5 (kN/m^3)
Atterberg Limits:	LL=69.2%, IP=40.5%

Table 2. Porto: Soil Details

Deposit:	Residual (Saprolite)
Lithology:	Silty clayey sand with some gravel
Soil structure from	Incomplete granite weathering
GWT, w_n , γ	-10/-12 m, 16/22.5 %, 16.6/20 kN/m^3
CF	3.3/9.5 %
Atterberg Limits:	LL=32/44 %, IP=5/17 %

Table 3. Porto: Pile Details

Pile Type:	Driven (C1) Precast	Bored (E9) Cased	Bored (T1) CFA
Material:	Concrete	Concrete	Concrete
Shape:	Square	Round	Round
Diameter (m):	0.35	0.60	0.60
Length (m):	6.0	6.0	6.0
Driving Date:	Sept.2003	-.-	-.-
Cast in situ Date:	-.-	Aug.2003	Aug.2003
SLT Date:	Jan.2004	Jan.2004	Jan.2004

To clarify the meaning of the parameters appearing in the graphs on Page 2, a specific glossary is reported in §9 with symbols, definition and reference equations, mainly derived from the CPT Guide (P.K. Robertson, 2015), the Manual of Subsurface Investigation (P.W. Mayne, 2001) and the CPT State of Practice Report (P.W. Mayne, 2007).

2 PILE CAPACITY DESIGN METHODS

Some CPT based, direct design methods (LCPC, Eslami&Fellenius, KTRI and Togliani), described by Niazi and Mayne (2013), were used to verify their sensitivity to the presence of a soil structure.
The latest version (Santa Cruz Prediction Event, 2017) of the mentioned Author's method, is the following:

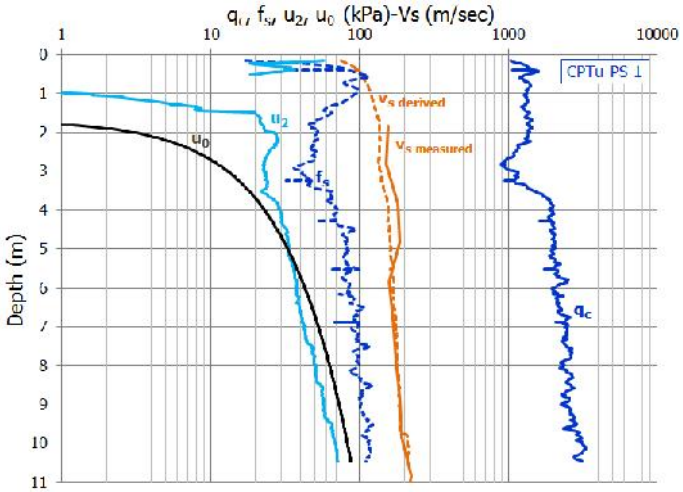

Figure 1. Merville: Guide Plot

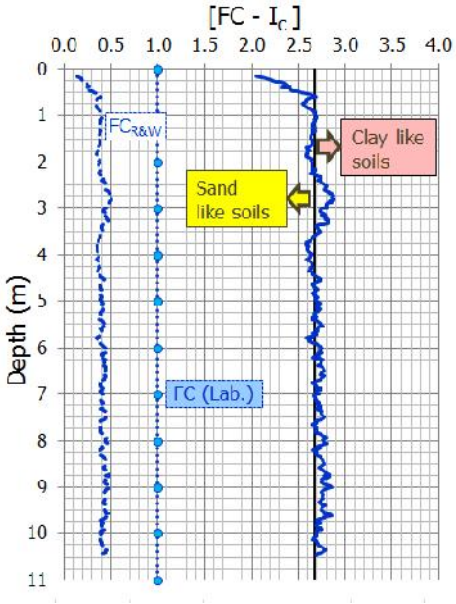

Figure 2. Merville: Soil Behaviour Plots

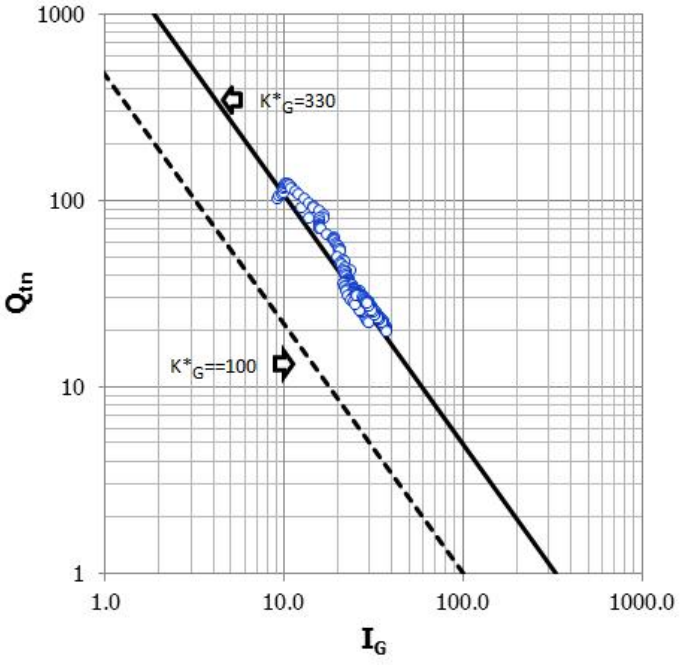

Figure 3. Merville K*G Plots

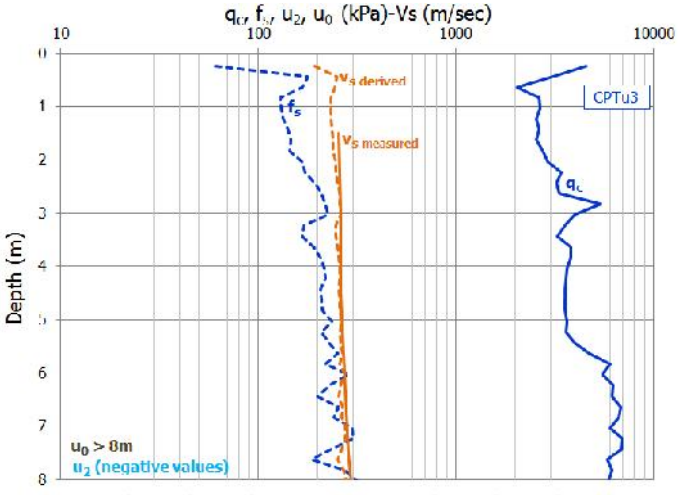

Figure 4. Porto: Guide Plots

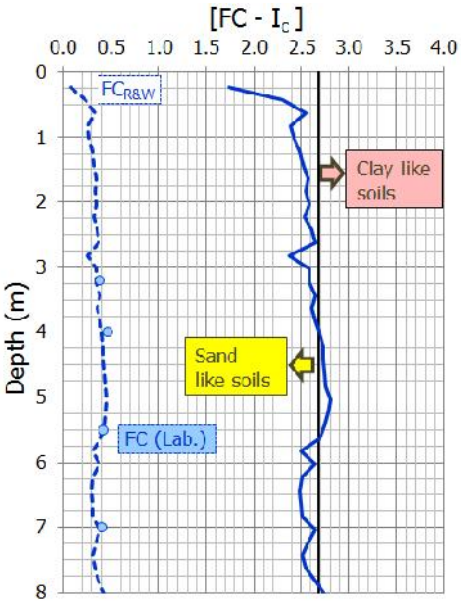

Figure 5. Porto: Soil Behaviour Plots

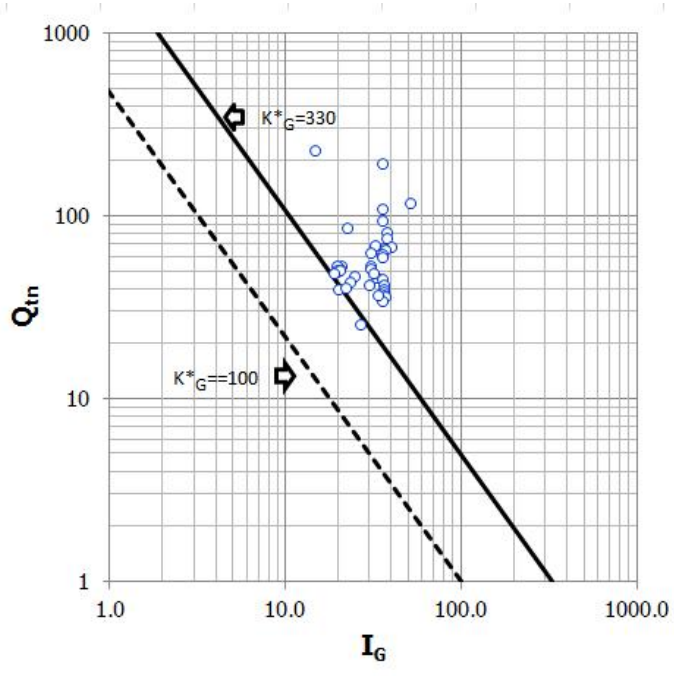

Figure 6. Porto K*G Plots

2.1 *Unit Friction (q_s)*

$$q_s=\beta\, q_c^{0.4} \quad \text{if } f_s\leq 20 \qquad (1)$$
$$q_s=\beta\{q_c^{0.52}[\,(0.4+LN(R_f)]\} \quad \text{if } R_f\geq 1.5 \qquad (2)$$
$$q_s=\beta\{q_c^{0.51}[0.8+(1-R_f)/8]\} \quad \text{if } 1\leq R_f<1.5 \qquad (3)$$
$$q_s=\beta\{q_c^{0.53}[0.8+(1.1-Rf)/8]\} \quad \text{if } R_f<1 \qquad (4)$$

2.2 *Unit Base (q_b)*

$$q_b=q_{c\ toe}[\lambda+(0.005Lpile/Dpile)] \qquad (5)$$

where $q_{c\ toe}$ goes from +8 dtoe to -4dtoe

Table 6 summarizes the corresponding Pile Type coefficients:

Table 6. β and λ coefficients

Pile Type	β	λ
Driven (precast/jacked)	1.00	0.30
Drill.Displacement.	0.90	0.25
Pipe (Open End)	0.70	0.20
CFA, Bored (cased-cohesionless, bentonite)	0.60	0.15
Bored (bentonite-upper bound)	0.60	0.10
Bored (cased- cohesive)	0.50	0.10
Bored (bentonite-lower bound)	0.40	0.05

The capacities derived from the four quoted methods were then compared with the ones calculated from the approach specified below, including the normalized rigidity index K^*_G.

2.3 *Unit friction (q_s)*

$$q_s=\beta q_c^{[0.3+\,x]} \qquad (6)$$

where $x=LOG(K^*_G{}^{\alpha})$

2.4 *Unit base (q_b): the same of § 2.2*

3 LOAD-MOVEMENT PREDICTION

The Chen & Kulhawy criterion (2002), shown in Figure 4, has been used to estimate the force-movement correlation for each pile and then the corresponding predicted curve, set via the Ratio Function.

According to this Function, the equation for unit resistance at a given movement in relation to the target resistance and target movement, is expressed by the following equation (B.Fellenius-Red Book):

$$r=r_{trg}\,(\delta/\delta_{trg})^{\theta} \qquad (7)$$

where r= variable force r_{trg} =target resistance
δ= var. movement δ_{trg} = movement at r_{trg}
θ=function coefficient ($0<\theta<1$)

The resistances derived with the new design method were considered as the target ones while the corresponding movement was set at s/d=10% to obtain a complete load-movement curve.

For Merville piles, the cohesive soil curve was taken as reference, while for Porto, the cohesionless soil curve was used (Figure 4).

The superposition between measured and predicted load-movement diagrams is obtained by adjusting the value of the ϑ coefficient within reasonable limits until a satisfying agreement was obtained; hence the theoretically evaluated curves are of Class C.

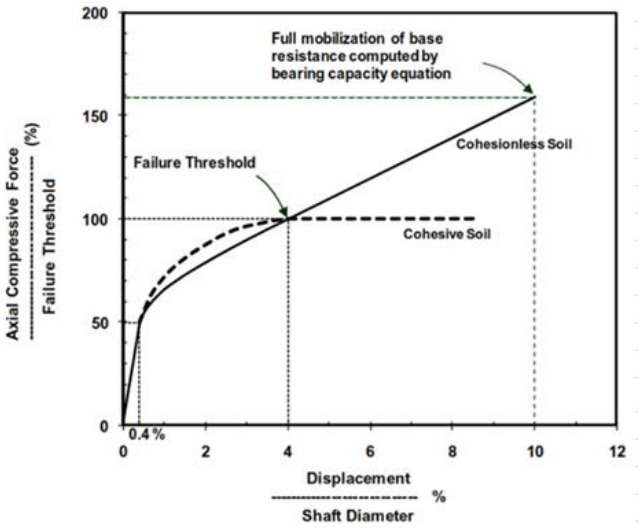

Figure 4. Chen & Kulhawy Criteria

4 MERVILLE PILE DESIGN

The capacities obtained with the several design methods considered are presented in Figure 5; Figure 6 shows the predicted load-movement curve, modeled using a function coefficient equal to 0.04.

Histograms in Figure 5 show the credible shaft resistance obtained with all the methods except for LCPC that, being only based on q_c, is unable to appreciate the improvement of subsoil characteristics due to the presence of microstructure.

The trend of the load-movement curves suggests that the toe capacity evaluated both with LCPC and Eslami&Fellenius methods could be overestimated.

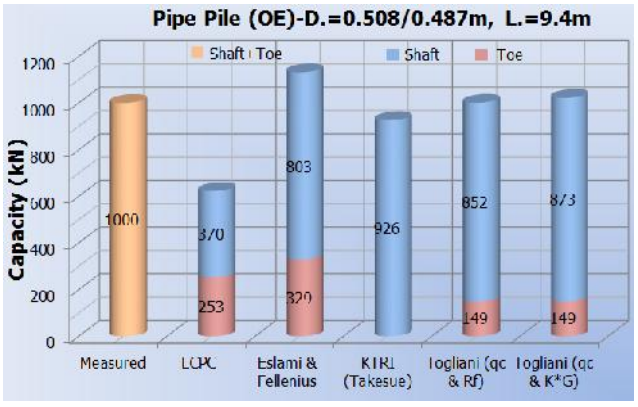

Figure 5. Pile Capacities Comparison

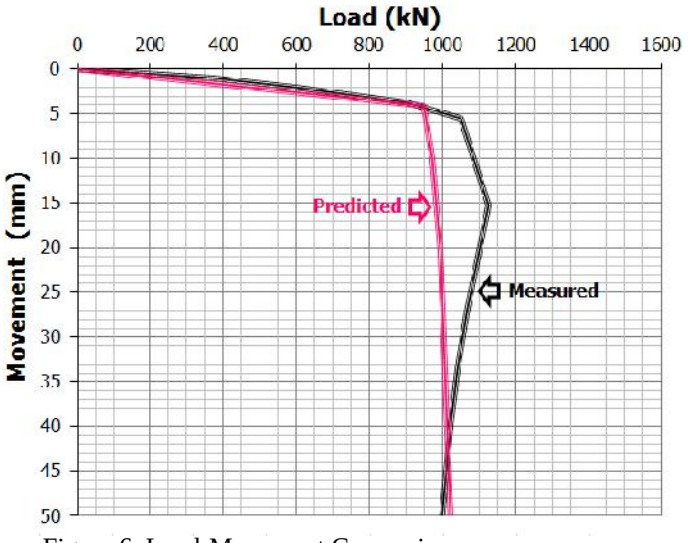

Figure 6. Load-Movement Comparison

5 PORTO PILES DESIGN

In this experimental site, the toe resistance was measured via strain gauges at a movement equal to s/d=10%, for pile E9 only, as represented in Figure 7.

The predicted load-movement curve (Figure 8) was assembled using function coefficients equal to 0.12 for shaft and 0.4 for toe resistance, respectively.

As previously noted, the LCPC shaft resistance is clearly inadequate as well as, in the opposite direction, the one obtained by KTRI (there is no difference between bored and driven piles!), while Eslami&Fellenius method was not considered, as more appropriate for driven piles

The design related to CFA Pile (T1) is summarized below and the notes concerning shaft resistance (Figure 9) are similar to the previous ones.

The function coefficient used for the predicted load-movement curve (Figure 10), this time has been set equal to 0.15.

Figure 11 shows the capacities of the driven precast pile (C1) and Figure 12, the load-movement curves.

To close on the predicted one, a function coefficient equal to 0.08 was used in this case, proving that shaft resistance is totally dominant.

Once again the LCPC shaft resistance is inadequate as well as the one derived from Eslami &Fellenius as the high f_s values are not balanced by consistent q_c values, in spite of the choice of unit frictions falling in the field with rather high shaft correlation coefficient (silty clay, silt).

The KTRI method, that for bored cased (E9) and CFA piles (T1) showed largely overestimated results, this time provides a consistent shaft resistance (clearly, now the non-difference between drilled and driven piles is reasonable).

About the new design method, it should be stressed that the prefabricated piles of both experimental sites seem, as expected, less performing (α=0.11) than those cast in place (α=0.10).

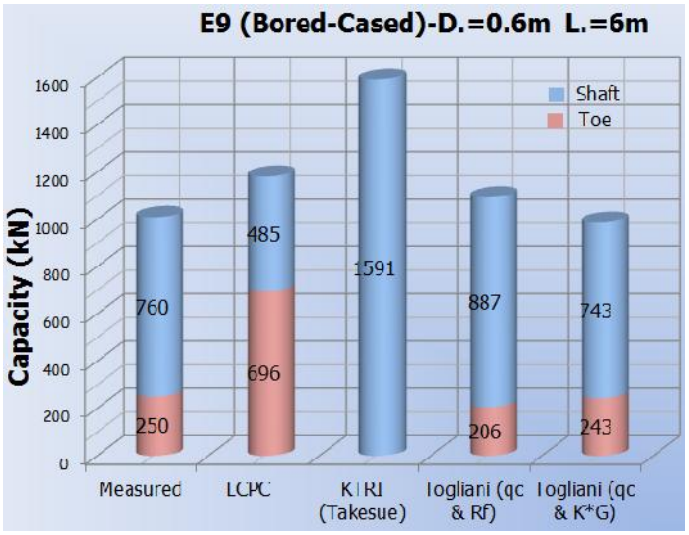

Figure 7. E9: Pile Capacities Comparison

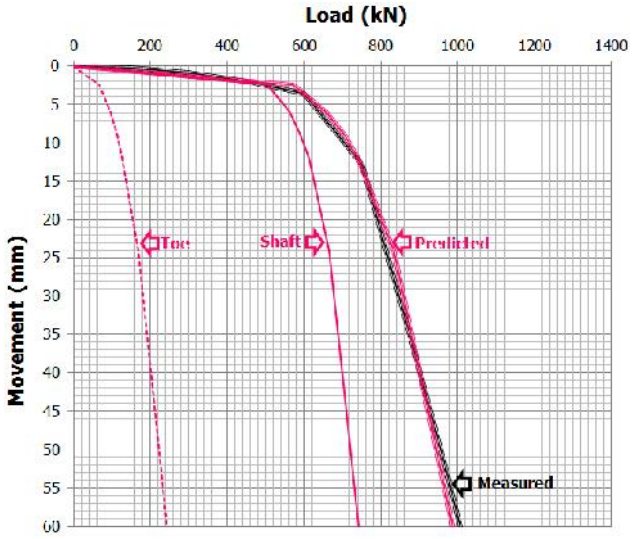

Figure 8. E9: Load-Movement Comparison

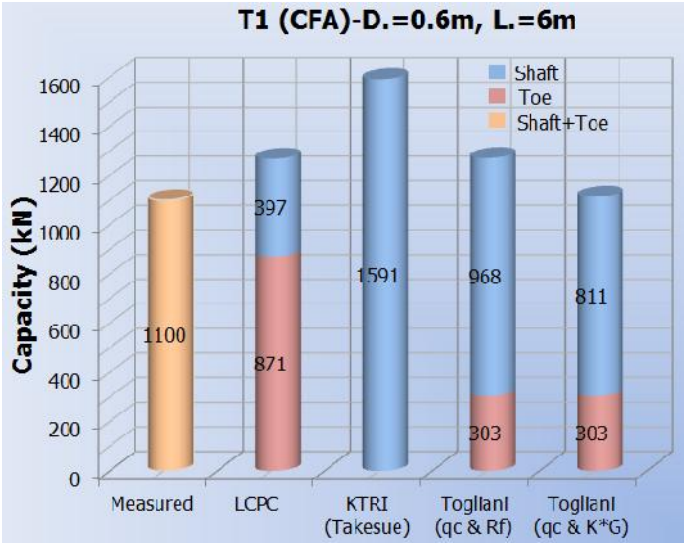

Figure 9. T1: Pile Capacities Comparison

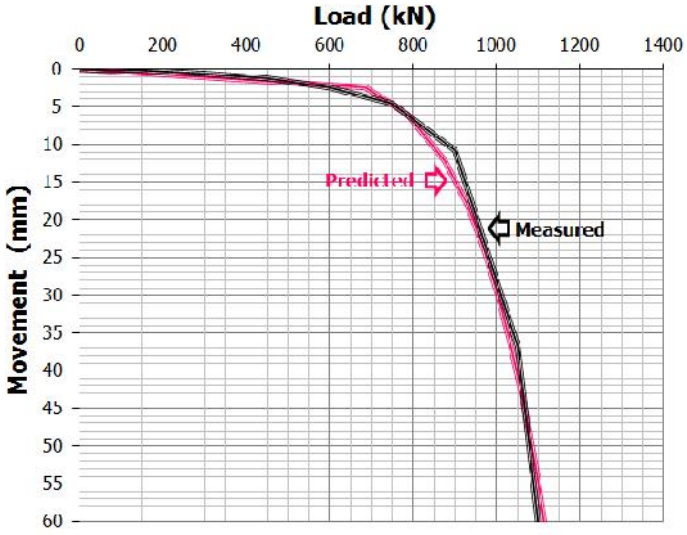

Figure 10. T1: Load-Movement Comparisons

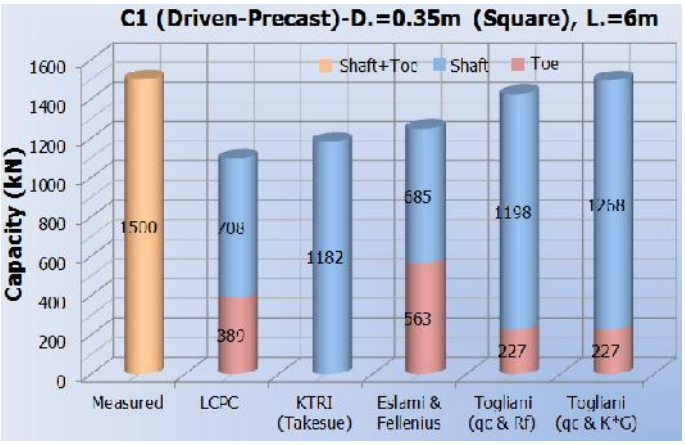

Figure 11. C1: Pile Capacities Comparison

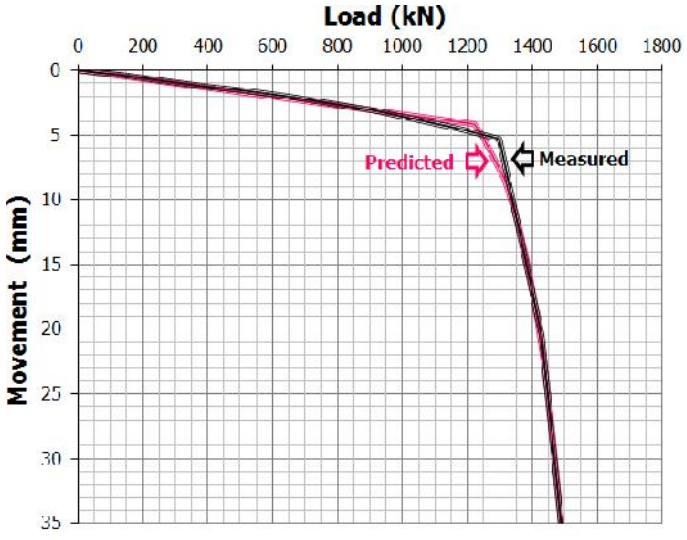

Figure 12. C1: Load-Movement Comparison

6 CONCLUSIONS

Cone resistance values are the most reliable among the measured CPTu parameters; however, as mentioned above, the sole consideration of q_c does not allow to understand the possible dilatant behaviour of the micro-structured soil. Hence, at least in these instances, the LCPC method becomes unreliable.

The design methods giving greater weight to f_s (KTRI and Eslami & Fellenius) provide good result in Merville because q_c and f_s values are mutually consistent.

On the contrary, this is not the case for Porto where very high f_s values (the silty sand soil retains a residual part of the parent rock structure), are unbalanced in comparison to q_c values.

While the shaft capacity predicted for the driven pile C1 with Eslami & Fellenius method is then inappropriate, for the same pile the one predicted using KTRI method, is adequate because its aforementioned ambivalence, at least in this case, is winning.

The Togliani method (2008/2017) that uses, jointly with q_c, also the friction ratio R_f , is less affected by the fluctuations in the f_s values; this is the reason why it provides very accurate pile capacity for Merville, remaining excellent (-5%) for pile C1 in Porto, good for pile E9 (+8%) and again sufficiently approximated for pile T1 (+16%) still located on the same site.

Finally, the newly proposed design method based on q_c and K^*_G values can be considered as self-adjusting with a good approximation to soils of different lithology and microstructural origin and proves to be promising; obviously, further confirmations are needed.

7 AKNOWLEDGMENT

Many thanks are addressed to Prof. P.K. Robertson, and to Dr. L. Albert for their critical review and suggestions.

8 REFERENCES

Chen, Y. J. and Kulhawy, F. H.2002. *Evaluation of drained axial capacity for drilled shafts.* Conference: International Deep Foundations Congress 2002.

Fellenius B.H.2017. *Basic of foundation design.* Red Book, Electronic Edition, January 2017

Fellenius B.H ,Terceros H.M.and Massarsch K.R.2017. *Bolivian experimental site for testing*. Proceedings 3rd International Conference on Deep Foundations. Santa Cruz 2017

Mayne P.W. 2001. *Manual on subsurface investigation.* FWHA, Washington DC.

Mayne, P.W.2007.NHRCP Project 20-05; Task 37-14: *Cone Penetration Testing -State-of Practice*.TRB

Niazi F.S.and Mayne P.W.2013.*Cone penetration test based direct methods for evaluating axial capacity of single piles.* Springer Science+Business Media Dordrecht 2013

P.K.Robertson.2015. *CPT Guide.* Electronic Edition

P.K.Robertson.2016. *Cone penetration test (CPT)- based soil behaviour type (SBT) classification system — an update*. Canadian Geotechnical Journal, 53(12)1910-1927

Togliani, G. 2008. *Pile capacity prediction for in situ tests.* Proceedings ISC-3 April 1-4, 2008. 1187-1192. Taylor & Francis Group, London, UK

9 GLOSSARY

z= depth
γ_n =natural unit weight
q_c= cone resistance
f_s= sleeve friction
u_2= pore pressure measured behind the cone
q_t =corrected cone resistance=$q_c+u_2(1-a)$
R_f= friction ratio=$(f_s/q_t)100$
σ_v= vertical stress= $z\gamma n$
u_0=hydrostatic pore pressure
σ'_v=effective vertical stress= σ_v-u_0
σ'_p=effective max. past vertical stress
OCR= overconsolidation ratio=σ'_p/σ'_v
q_{tn}=net corrected cone resistance=$q_t-\sigma_v$
Q_{tn}= normalized cone resistance=$[(q_t-\sigma_v)/P_a][P_a/\sigma'_v]^n$
I_c= classification index (P.K. Robertson)
$FC_{R\&W}$= Fine content (Robertson & Wride)
I_c >3.5 FC=1, 1.31<I_c<3.5 FC=1.75$I_c^{3.25}$-3.7, I_c<1.31 FC=0
CF= Clay Fraction
Vs=shear wave velocity
V_s derived (Porto)=118.8LOG(f_s)-18.5 (P.W. Mayne)
V_s derived (Merville)-Baldi (1992) mod. Togliani=
$277q_c^{0.12}\sigma'^{0.18}_v$ if σ'_v<100 kPa otherwise = $277\ qc^{0.13}\sigma'^{0.22}_v$
G_0= maximum .shear modulus =ρV_s^2
I_G= small-strain rigidity index =(G_0/q_{tn})
K^*_G=normalized small-strain rigidity index=$Q_{tn}^{0.75}I_G$